

1 LEVERAGING MULTI-MESSENGER ASTROPHYSICS FOR DARK MATTER SEARCHES

By

Daniel Nicholas Salazar-Gallegos

A DISSERTATION

Submitted to  
Michigan State University  
in partial fulfillment of the requirements  
for the degree of

Physics—Doctor of Philosophy  
Computational Mathematics in Science and Engineering—Dual Major

Today

**ABSTRACT**

3 I did Dark Matter with HAWC and IceCube. I also used Graph Neural Networks

<sup>4</sup> Copyright by

<sup>5</sup> DANIEL NICHOLAS SALAZAR-GALLEGOS

<sup>6</sup> Today

## ACKNOWLEDGMENTS

8 I love my friends. Thanks to everyone that helped me figure this out. Amazing thanks to the people  
9 at LANL who supported me. Eames, etc Dinner Parties Jenny and her child Kaydince Kirsten, Pat,  
10 Andrea Family. You're so far but so critical to my formation. Unconditional love. Roommate

## TABLE OF CONTENTS

12	LIST OF TABLES . . . . .	vi
13	LIST OF FIGURES . . . . .	vii
14	LIST OF ABBREVIATIONS . . . . .	ix
15	CHAPTER 1      INTRODUCTION . . . . .	1
16	CHAPTER 2      DARK MATTER IN THE COSMOS . . . . .	2
17	2.1 Introduction . . . . .	2
18	2.2 Dark Matter Basics . . . . .	3
19	2.3 Evidence for Dark Matter . . . . .	4
20	2.4 Searching for Dark Matter . . . . .	11
21	2.5 Sources for Indirect Dark Matter Searches . . . . .	16
22	2.6 Multi-Messenger Dark Matter . . . . .	18
23	CHAPTER 3      DETECTING HIGH ENERGY NEUTRAL MESSENGERS . . . . .	21
24	3.1 Cherenkov Radiation . . . . .	21
25	3.2 HAWC . . . . .	21
26	3.3 IceCube . . . . .	21
27	3.4 Opportunities to Combine for Dark Matter . . . . .	21
28	CHAPTER 4      HIGH ALTITUDE WATER CHERENKOV (HAWC) OBSERVATORY . . . . .	22
29	4.1 The Detector . . . . .	22
30	4.2 Events Reconstruction and Data Acquisition . . . . .	22
31	4.3 Remote Monitoring . . . . .	22
32	CHAPTER 5      ICECUBE NEUTRINO OBSERVATORY . . . . .	23
33	5.1 The Detector . . . . .	23
34	5.2 Events Reconstruction and Data Acquisition . . . . .	23
35	5.3 Northern Test Site . . . . .	23
36	CHAPTER 6      COMPUTATIONAL TECHNIQUES IN PARTICLE ASTROPHYSICS . . . . .	24
37	6.1 Neural Networks for Gamma/Hadron Separation . . . . .	24
38	6.2 Parallel Computing for Dark Matter Analyses . . . . .	24
39	CHAPTER 7      GLORY DUCK . . . . .	25
40	CHAPTER 8      NU DUCK . . . . .	26
41	BIBLIOGRAPHY . . . . .	27

42

## **LIST OF TABLES**

43

Proof I know how to include

## LIST OF FIGURES

45	Figure 2.1	Rotation curve fit to NGC 6503 from [7]. Dashed line is the contribution 46 from visible matter. Dotted curves are from gas. Dash-dot curves are from 47 dark matter (DM). Solid line is the composite contribution from all matter 48 and DM sources. Data are indicated with bold dots with error bars. Data 49 agree strongly with matter + DM composite prediction . . . . .	5
50	Figure 2.2	Light from distant galaxy is bent in unique ways depending on the distribution 51 of mass between the galaxy and Earth. Yellow dashed lines indicate where 52 the light would have gone if the matter were not present [8]. . . . .	7
53	Figure 2.3	(left) Optical image of galactic cluster. (right) X-ray image of the cluster with 54 redder meaning hotter and higher baryon density. (both) Green contours are 55 reconstruction of gravity contours from micro-lensing. White rings are the 56 best fit mass maxima at 68.3%, 95.5%, and 99.7% confidence. The maxima 57 of the clusters are clearly separated from x-ray maxima. [10] . . . . .	8
58	Figure 2.4	Plank CMB sky. Sky map features small variations in temperature in pri- 59 mordial light. These anisotropies can be used to make inferences about the 60 universe's energy budget. [11] . . . . .	9
61	Figure 2.5	Observed Cosmic Microwave Background power spectrum as a function of 62 multipole momentfrom Plank [11]. Blue line is best fit model from $\Lambda$ CDM. 63 Red points and lines are data and error respectively. . . . .	10
64	Figure 2.6	Predicted power spectra of CMB for different $\Omega_m h^2$ values. (left) Low $\Omega_m h^2$ 65 increases the prominence of first and second peaks. (middle) $\Omega_m h^2$ is most 66 similar to the observed power spectrum. The second and third peaks are 67 similar in height. (right) $\Omega_m h^2$ is large which suppresses the first peak and 68 raises the prominence of the third peak. . . . .	10
69	Figure 2.7	The Standard Model (SM) of particle physics. Figure taken from <a href="http://www.quantumdiaries.org/2014/03/14/the-standard-model-a-beautiful-but-flawed-theory/">http://www.quantumdiaries.org/2014/03/14/the-standard-model-a-beautiful-but-flawed-theory/</a> . . . . .	12
72	Figure 2.8	Simplified Feynman diagram demonstrating with different ways DM can 73 interact with SM particles. The 'X's refer to the DM particles whereas the 74 SM refer to fundamental particles in the SM. The large circle in the center 75 indicates the vertex of interaction and is purposely left vague. The colored 76 arrows refer to different directions of time as well as their respective labels. 77 The arrows indicate the initial and final state of the DM -SM interaction in time.	13

78	Figure 2.9 A single jet event in ATLAS detector from 2017 [16]. Jet momentum observed 79 to be 1.9 TeV. Missing transverse momentum observed to be 1.9 TeV as the 80 initial momentum of the event was 0. Implied MET is shown as a red dashed 81 line in event display. . . . .	14
82	Figure 2.10 More detailed pseudo-Feynman diagram of particle cascade from dark matter 83 annihilation into 2 quarks. The quarks hadronize and decay to stable particles 84 like $\gamma$ or the anti-proton ( $p^-$ ). Diagram pulled from ICRC 2021 presentation 85 on DM annihilation search [17]. . . . .	15
86	Figure 2.11 Dark Matter (DM) decay spectrum for $b\bar{b}$ initial state and $\gamma$ final state. Redder 87 spectra are for larger DM masses. Bluer spectra are light DM masses. $x$ is a 88 unitless factor defined as the ratio of the mass of DM, $m_\chi$ , and the final state 89 particle energy $E_\gamma$ . Figure from [19]. . . . .	17
90	Figure 2.12 Different dark matter density profiles compared. Some models produce very 91 large densities at small r [20]. . . . .	18
92	Figure 2.13 The Milky Way Galaxy in photons ( $\gamma$ ) and neutrinos ( $\nu$ ) [22]. Galactic center 93 is at $l=0^\circ$ and is the brightest region in all panels. (top) An Optical color image 94 of the Milky Way galaxy seen from Earth. Clouds of gas and dust obscure 95 some of the light from stars. (2nd down) Integrated flux of $\gamma$ -rays observed 96 by the Fermi-LAT telescope [23]. (middle) Expected neutrino emission 97 that corresponds with Fermi-LAT observations. (2nd up) Expected neutrino 98 emission profile after considering detector systematics of IceCube. (bottom) 99 Observed neutrino emission from region of the galactic plane. Substantial 100 neutrino emission is detected. . . . .	19
101	Figure 2.14 Dark Matter annihilation spectra for different final state particle and standard 102 model annihilation channels [24]. Photons (red), $e^\pm$ (green), $\bar{p}$ (blue), $\nu$ (black). . . . .	20

103

## LIST OF ABBREVIATIONS

- 104 **MSU** Michigan State University  
105 **LANL** Los Alamos National Laboratory  
106 **DM** Dark Matter  
107 **SM** Standard Model  
108 **HAWC** High Altitude Water Cherenkov Observatory

109

## CHAPTER 1

### INTRODUCTION

110 Is the text not rendering right? Ah ok it knows im basically drafting the doc still

## CHAPTER 2

111

### DARK MATTER IN THE COSMOS

112 **2.1 Introduction**

113 I will attempt to explain the dark matter problem at an entry level with the following thought  
114 experiment. Imagine you are the teacher for an elementary school classroom. You take them on a  
115 field trip to your local science museum and among the exhibits is one for mass and weight. The  
116 exhibit has a gigantic scale, and you produce a fun problem for your classroom.

117 You ask your class, "What is the total weight of the classroom? Give your best estimation to  
118 me in 30 minutes, and then we'll check your guess on the scale. If your guess is within 10% of the  
119 right answer, we will stop for ice cream on the way back"

120 The students are ecstatic to hear this, and they get to work. The solution is some variation of  
121 the following strategy. The students should give each other their weight or best guess if they do  
122 not know. Then, all they must do is add each student's weight and get a grand total for the class.  
123 The measurement on the giant scale should show the true weight of the class. When comparing the  
124 measured weight, multiply the observation by 1.1 and 0.9 to get the +/- 10% tolerance, respectively.

125 Two of your students, Sandra and Mario, return to you with a solution.

126 They say, "We weren't sure of everyone's weight. We used 65 lbs. for the people we didn't  
127 know and added everyone who does know. There are 30 of us, and we got 2,000 lbs.! That's a ton!"

128 You estimated 1,900 lbs. assuming the average weight of a student in your class was 60 lbs.  
129 So, you are pleased with Sandra's and Mario's answer. You instruct your students to all gather on  
130 the giant scale and read off the weight together. To all your surprise, the scale reads *10,000 lbs.!*  
131 10,000 is significantly more than a 10% error from 2,000. In fact, it is approximately 5 times more  
132 massive than either your or your students' estimates. You think to yourself and conclude there  
133 must be something wrong with the scale. You ask an employee to check the scale and verify it is  
134 calibrated well. They confirm that the scale is in working order. You weigh a couple of students  
135 individually to test that the scale is well calibrated. Sandra weighs 59 lbs., and Mario weighs 62  
136 lbs., typical weights for their age. You then weigh each student individually and see that their

137 weights individually do not deviate greatly from 60 lbs. So, where does all the extra weight come  
138 from?

139 This thought experiment serves as an analogy to the Dark Matter problem. The important  
140 substitution to make however is to replace the students with stars and the classroom with a galaxy,  
141 say the Milky Way. Individually the mass of stars is well measured and defined with the Sun as our  
142 nearest test case. However, when we set out to measure the mass of a collection of stars as large as  
143 galaxies, our well-motivated estimation is wildly incorrect. There simply is no way to account for  
144 this discrepancy except without some unseen, or dark, contribution to mass and matter in galaxies.  
145 I set out in my thesis to narrow the possibilities of what this Dark Matter could be.

146 This chapter is organized like the following... **TODO: Text should look like ... Chaper x has**  
147 **blah blah blah.**

## 148 2.2 Dark Matter Basics

149 Presently, the most compelling Dark Matter (DM) model is  $\Lambda$  Cold Dark Matter, or  $\Lambda$ CDM. I  
150 present the evidence supporting  $\Lambda$ CDM in 2.3, yet discuss the conclusions of the  $\Lambda$ CDM model  
151 here. According to  $\Lambda$ CDM fit to observations on the Cosmic Microwave Background (CMB), DM  
152 is 26.8% of the universe's current energy budget Baryonic matter, stuff like atoms, gas, and stars,  
153 contributes to 4.9% of the universe's current energy budget [1, 2, 3].

154 DM is dark; it does not interact readily with light at any wavelength. DM also does not interact  
155 noticeably with the other standard model forces (Strong and Weak) at a rate that is readily observed  
156 [3]. DM is cold, which is to say that the average velocity of DM is below relativistic speeds [1].  
157 'Hot' DM would not likely manifest the dense structures we observe like galaxies, and instead  
158 would produce much more diffuse galaxies than what is observed [3, 1]. DM is old; it played a  
159 critical role in the formation of the universe and the structures within it [1, 2].

160 Observations of DM have so far been only gravitational. The parameter space available to  
161 what DM could be therefore is extremely broad. Searches for DM are summarized by supposing  
162 a hypothesis that has not yet been ruled out and performing measurements to test them. When  
163 the observations yield a null result, the parameter space is further constrained. I present some

164 approaches for DM searches in Section 2.4.

165 **2.3 Evidence for Dark Matter**

166 Dark Matter (DM) has been a looming problem in physics for almost 100 years. Anomalies  
167 have been observed in galactic dynamics as early as 1933 when Fritz Zwicky noticed unusually  
168 large velocity dispersions in the Coma cluster. Zwicky's measurement was the first recorded to  
169 use the Virial theorem to measure the mass fraction of visible and invisible matter in celestial  
170 bodies [4]. From Zwicky in [5], "*If this would be confirmed, we would get the surprising result*  
171 *that dark matter is present in much greater amount than luminous matter.*" Zwicky's and others'  
172 observation did not instigate a crisis in astrophysics because the measurements did not entirely  
173 conflict with their understanding of galaxies [4]. In 1978, Rubin, Ford, and Norbert measured  
174 rotation curves for ten spiral galaxies [6]. Rubin et. al.'s 1978 publication presented a major  
175 challenge to the conventional understanding of galaxies that could no longer be accredited to  
176 measurement uncertainties. Evidence has been mounting ever since for this exotic form of matter.  
177 The following subsections sample some of the compelling evidence supporting DM.

178 **2.3.1 First Clues: Stellar Velocities**

179 Zwicky's, and later Rubin's, measurements of the stellar velocities were built upon the Virial  
180 theorem, shown as

$$2T + V = 0. \quad (2.1)$$

181 Where  $T$  is the kinetic energy and  $V$  is the potential energy in a self-gravitating system. The  
182 potential was defined as the classical Newton's law of gravity from stars and gas contained in the  
183 observed galaxies

$$V = -\frac{1}{2} \sum_i \sum_{j \neq 1} \frac{m_i m_j}{r_{ij}}. \quad (2.2)$$

184 Zwicky et. al. measured just the velocities of stars apparent in optical wavelengths [5]. Rubin et.  
185 al. added by measuring the velocity of the hydrogen gas via the 21 cm emission line of Hydrogen  
186 [6]. The velocities of the stars and gas are used to infer the total mass of galaxies and galaxy clusters  
187 via Eq. (2.1). An inferred mass is also made from the luminosity of the selected sources. The two

188 inferences are compared to each other as a luminosity to mass ratio and typically yields [1]

$$\frac{M}{L} \sim 400 \frac{M_{\odot}}{L_{\odot}} \quad (2.3)$$

189  $M_{\odot}$  and  $L_{\odot}$  referring to stellar mass and stellar luminosity, respectively. These ratios clearly indicate  
190 a discrepancy in apparent light and mass from stars and gas and their velocities.

191 Rubin et.al. [6] demonstrated that the discrepancy was unlikely to be an under-estimation of  
192 the mass of the stars and gas. The inferred 'dark' mass was up to 5 times more than the luminous  
193 mass. This dark mass also needed to extend well beyond the extent of the luminous matter.

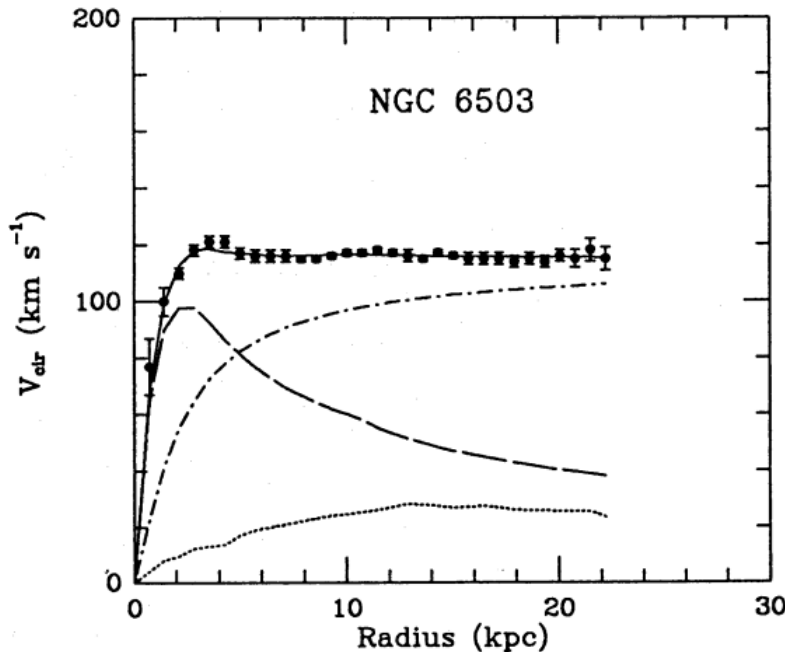


Figure 2.1 Rotation curve fit to NGC 6503 from [7]. Dashed line is the contribution from visible matter. Dotted curves are from gas. Dash-dot curves are from dark matter (DM). Solid line is the composite contribution from all matter and DM sources. Data are indicated with bold dots with error bars. Data agree strongly with matter + DM composite prediction

194 Fig. 2.1: features one of many observations made on the stellar velocities within galaxies.  
195 The measured rotation curves mostly feature a flattening of velocities at higher radius which is  
196 not expected if the gravity was only coming from gas and luminous matter. The extension of  
197 the flat velocity region also indicates that the DM is distributed far from the center of the galaxy.  
198 Modern velocity measurements include significantly larger objects, galactic clusters, and smaller

199 objects, dwarf galaxies. Yet, measurements along this regime are leveraging the Virial theorem  
200 with Newtonian potential energies. We know Newtonian gravity is not a comprehensive description  
201 of gravity. New observational techniques have been developed since 1978, and those are discussed  
202 in the following sections.

203 **2.3.2 Evidence for Dark Matter: Micro-lensing**

204 Modern evidence for dark matter comes from new avenues beyond stellar velocities. Gravita-  
205 tional micro-lensing from DM is a new channel from general relativity. The Cosmic Microwave  
206 Background shows that the universe had DM in it from an incredibly early stage. Computational  
207 resources have expanded in recent decades enabling universe models that again support the need  
208 for DM in the evolution of the universe.

209 General relativity predicts aberrations in light caused by massive objects. In recent decades  
210 we have been able to measure the lensing effects from compact objects and DM haloes. Fig. 2.2  
211 shows how different compact bodies change the final image of a faraway galaxy resulting from  
212 gravitational lensing. Gravitational lensing developed our understanding of dark matter in two  
213 important ways.

214 First, micro-lensing observations, or the lack of them, of our Milky Way halo resulted in a  
215 conspicuous absence of massive astrophysical compact halo objects (MACHOs). The hypothesis  
216 was that 'dark matter' could be accounted for by sufficiently dim compact objects. Such objects  
217 include things like planets, brown dwarves, black holes, or neutron stars. Whenever these objects  
218 passed in front of a large luminous source, such as the Large Magellenic Clouds, a variation in light  
219 should be observed [4]. The MACHO and EROS collaborations performed this observation and  
220 did not find a substantial contribution to the DM Milky Way halo from MACHOs. They measured  
221 that MACHOs of mass range 0.15 to  $0.9 M_{\odot}$  contributes to an upper limit of 8% of the DM halo  
222 mass [9].

223 Gravitational lensing can also be applied towards galaxy clusters for DM searches. The obser-  
224 vation of two merging galactic clusters in 2006, shown in Fig. 2.3, provided a compelling argument  
225 for particle DM outside the Standard Model. These clusters merged recently in astrophysical time

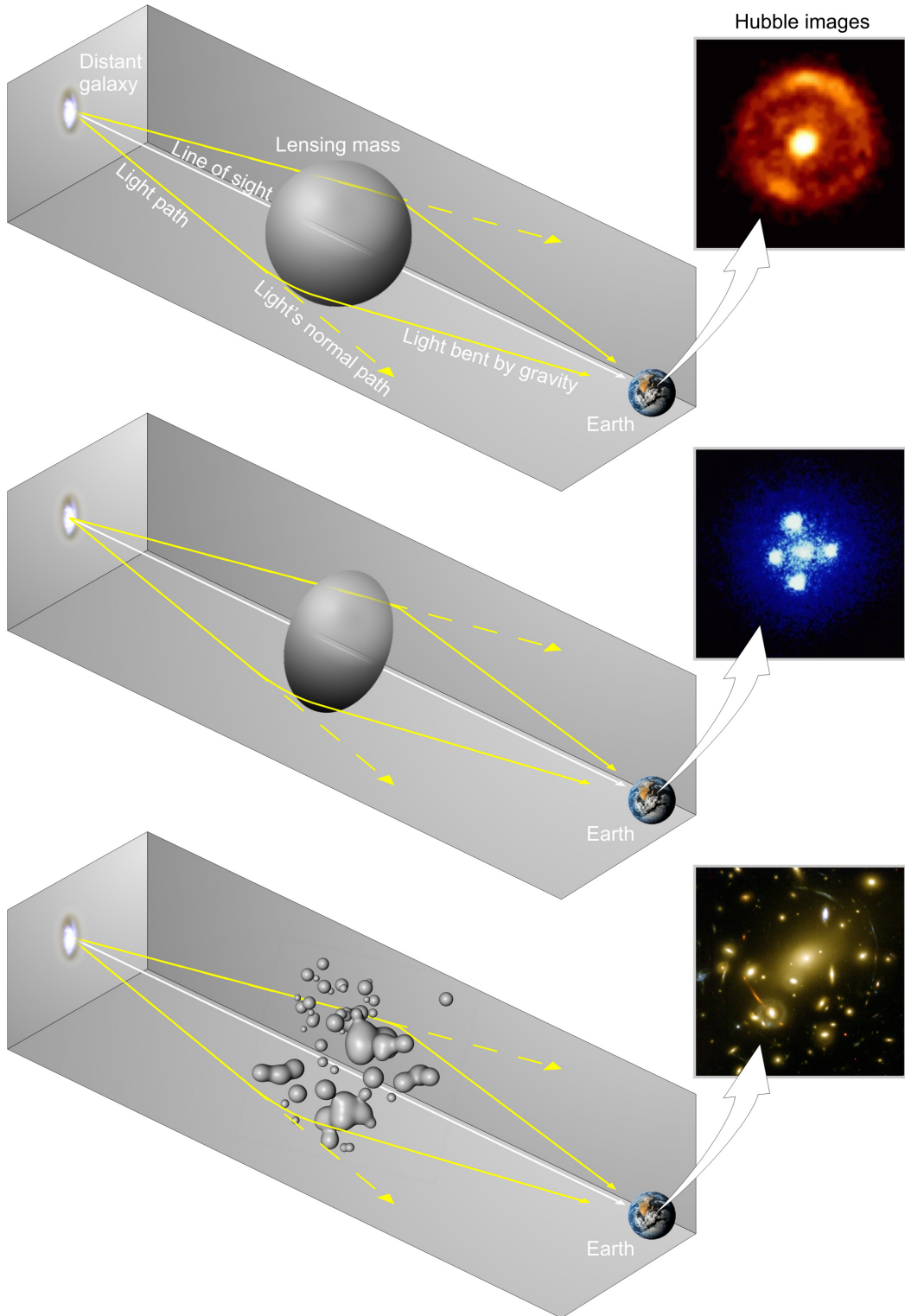


Figure 2.2 Light from distant galaxy is bent in unique ways depending on the distribution of mass between the galaxy and Earth. Yellow dashed lines indicate where the light would have gone if the matter were not present [8].

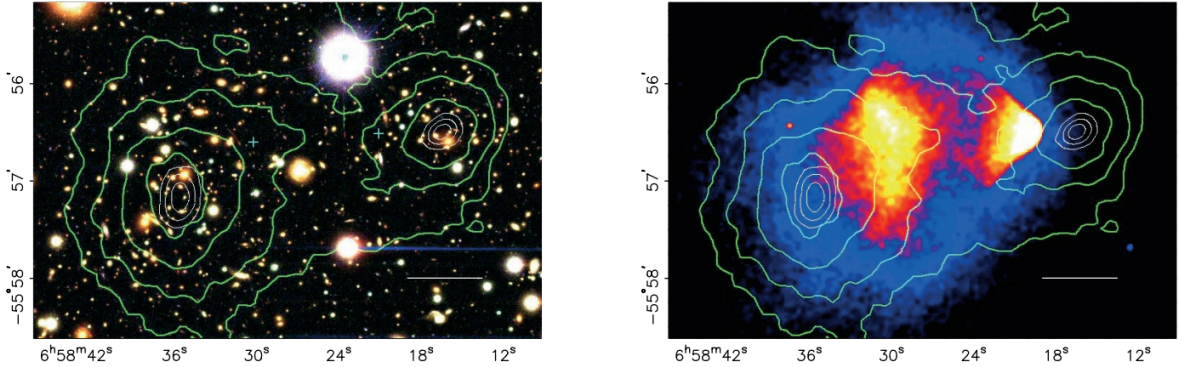


Figure 2.3 (left) Optical image of galactic cluster. (right) X-ray image of the cluster with redder meaning hotter and higher baryon density. (both) Green contours are reconstruction of gravity contours from micro-lensing. White rings are the best fit mass maxima at 68.3%, 95.5%, and 99.7% confidence. The maxima of the clusters are clearly separated from x-ray maxima. [10]

226 scales. Their recent merger separated the stars and galaxies are separated from the intergalactic  
 227 gas. For these clusters, the hot, intergalactic gas is responsible for most of the mass in the systems  
 228 [4]. The hot gas is observed from its x-rays argument. Two observations of the clusters were made  
 229 independently of each other. The first was the microlensing of light around the galaxies due to  
 230 their gravitational influences. When celestial bodies are large enough, the gravity they exert bends  
 231 space and time itself. These bending effects light and will deflect light an analogous way to how  
 232 lenses will bend light. With a sufficient understanding of light sources behind a celestial body, we  
 233 can reconstruct the contours of the gravitational lenses. The gradient of the contours then indicates  
 234 how dense the matter is and where it is.

235 The x-ray emission can then be observed from the clusters. Since these galaxies are mostly gas  
 236 and are merging, then the gas should be getting hotter. If they are merging, the x-ray emissions  
 237 should be the strongest where the gas is mostly moving through each other. Hence, X-ray emission  
 238 maps out where the gas is in the merging galaxy cluster.

239 The micro-lensing and x-ray observations were done on the Bullet cluster featured on Fig. 2.3.  
 240 The x-ray emmisions does not align with the gravitational countours from microlensing. The  
 241 incongruence in mass density and baryon density suggests that there is a lot of matter somewhere  
 242 that does not interact with light. Moreover, this dark matter is can not be baryonic [10]. The Bullet

243 Cluster measurement did not really tell us what DM is exactly, but it did give the clue that DM also  
244 does not interact with itself very strongly. If DM did interact strongly with itself, then it would  
245 have been more aligned with the x-ray emmision [10]. There have been follow-up studies of galaxy  
246 clusters with similar results. The Bullet Cluster and others like it provide a strong case against  
247 something possibly amiss in our gravitational theories.

248 **2.3.3 Evidence for Dark Matter: Cosmic Microwave Background**

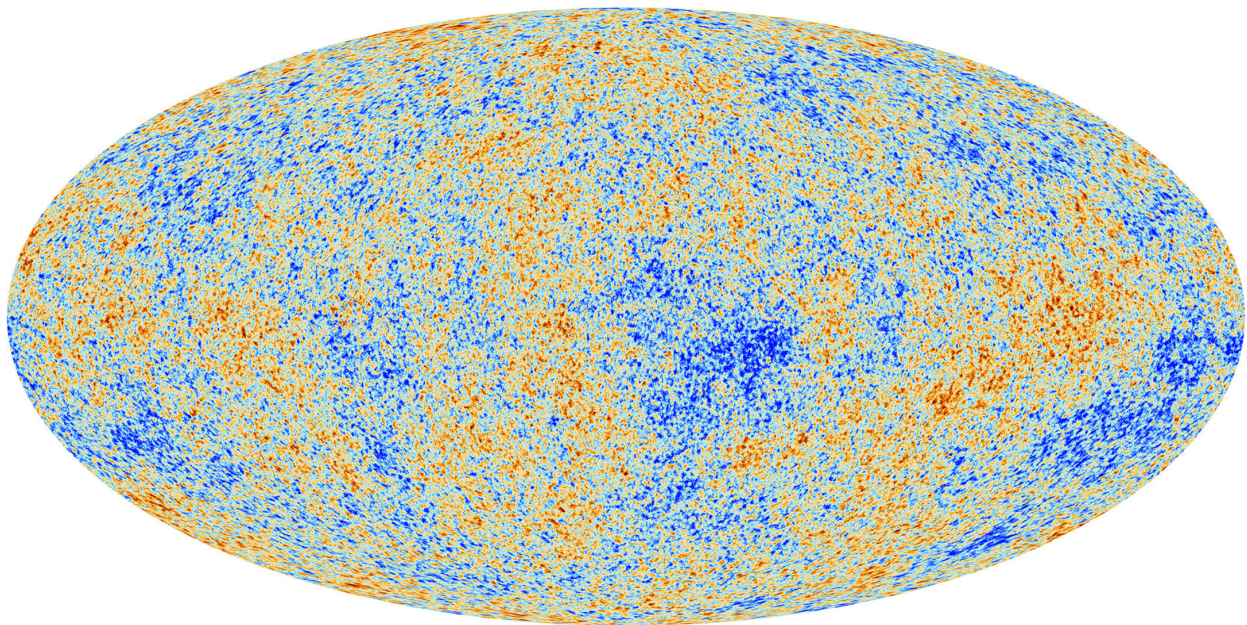


Figure 2.4 Plank CMB sky. Sky map features small variations in temperature in primordial light. These anisotropies can be used to make inferences about the universe's energy budget. [11]

249 The Cosmic Microwave Background (CMB) is the primordial light from the early universe  
250 when Hydrogen atoms formed from the free electron and proton soup in the early universe. The  
251 CMB is the earliest light we can observe; released when the universe was about 380,000 years old.  
252 Then we look at how the simulated universes look like compared to what we see. Fig. 2.4 is the  
253 most recent CMB image from the Plank observatory [11]. Redder regions indicate a slightly hotter  
254 region of the early universe and blue indicates colder.

255 To measure the DM, Dark Energy, and matter fractions of the universe from the CMB, the image  
256 is deconstructed into a power spectrum versus spherical multipole moments.  $\Lambda$ CDM provides the

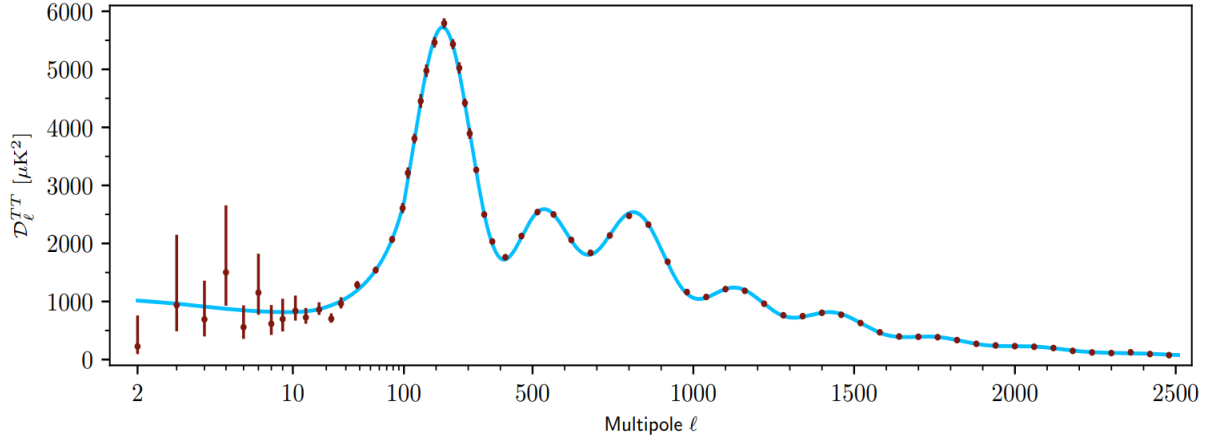


Figure 2.5 Observed Cosmic Microwave Background power spectrum as a function of multipole moment from Plank [11]. Blue line is best fit model from  $\Lambda$ CDM. Red points and lines are data and error respectively.

257 best fit to the power spectra of the CDM as shown in Fig. 2.5. The CMB power spectrum is very  
 258 sensitive to the fraction of each energy contribution in the early universe. Low  $l$  modes are dominated  
 259 by variations in gravitational potential. Intermediate  $l$  emerge from oscillations in photon-baryon  
 260 fluid from competing baryon pressures and gravity. High  $l$  is a damped region from the diffusion  
 261 of photons during electron-proton recombination. [1]

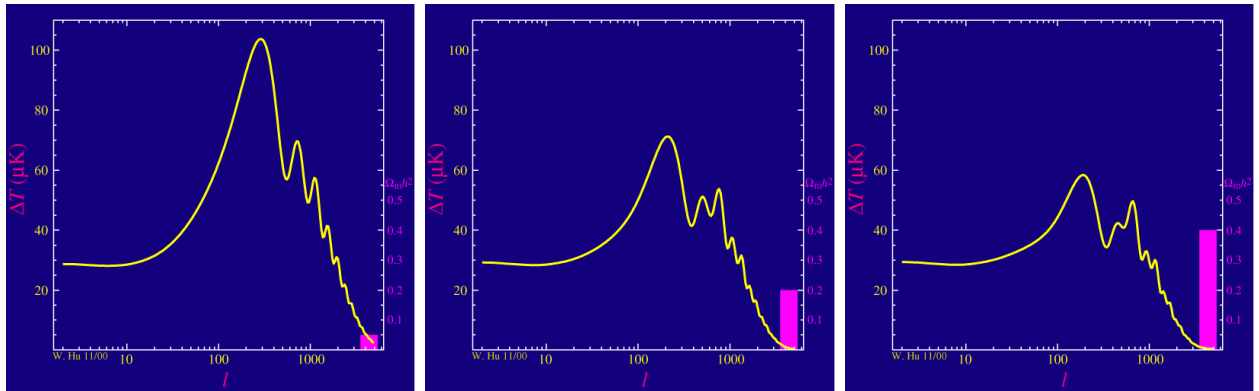


Figure 2.6 Predicted power spectra of CMB for different  $\Omega_m h^2$  values. (left) Low  $\Omega_m h^2$  increases the prominence of first and second peaks. (middle)  $\Omega_m h^2$  is most similar to the observed power spectrum. The second and third peaks are similar in height. (right)  $\Omega_m h^2$  is large which suppresses the first peak and raises the prominence of the third peak.

262 The harmonics would look very different for a universe with less DM. Fig. 2.6 shows the  
 263 differences expected in the power spectrum for different baryon fractions of the universe's energy

264 budget. The observations fit well with the  $\Lambda$ CDM model and the derived fractions are as follows.  
265 The matter fraction:  $\Omega_m = 0.3153$ ; and the baryon fraction:  $\Omega_b = 0.04936$  [11]. These findings  
266 do rely however on a few assumptions and the precision of the Hubble constant,  $H_0$ .  $H_0$  especially  
267 has seen a growing tension in recent decades that continues to deepened with observatories like the  
268 James Webb Telescope [12, 13]

269 Overall these observations form a compelling body of research in favor of dark matter. However,  
270 these observations really only confirm that DM is there. It takes another leap of theory and  
271 experimentation to make observations of DM that are non-gravitational in nature. One hypothesis  
272 is the Weakly Interacting Massive Particle DM. This DM candidate theory is discussed further in  
273 the next section and is the hypothesis to this thesis.

## 274 2.4 Searching for Dark Matter

275 There remains many options available to what Dark Matter could be. For a particle dark matter  
276 hypothesis, we assume that DM interacts in some way, even if very weakly, with the Standard  
277 Model (SM), see Section 2.4. The current status of the SM does not have a viable DM candidate.  
278 When looking at the standard model, we can immediately exclude any charged particle. This is  
279 because charged particles interact with light. If DM is charged, it would be immediately visible if  
280 it had similar charge to many SM particles. Specifically this will rule out the following charged,  
281 fundamental particles:  $e, \mu, \tau, W, u, d, s, c, t, b$  and their corresponding antiparticles. Recalling  
282 from earlier that DM must be long lived and stable over the age of the universe, this would exclude  
283 all SM particles with decay half-lives at or shorter than the age of the universe. The lifetime  
284 constraint additionally eliminates the  $Z$  and  $H$  bosons. Finally, the candidate DM needs to be  
285 somewhat massive. Recall from Section 2.2 that DM is cold or not relativistic through the universe.  
286 This eliminates the remaining SM particles:  $\nu_{e,\mu,\tau}, g, \gamma$  as DM candidates. Because there are no  
287 DM candidates within the SM, the DM problem strongly hints to physics beyond the SM (BSM).

### 288 2.4.1 Shake it, Break it, Make it

289 When considering DM that couples in some way with the SM, the interactions are roughly  
290 demonstrated by interaction demonstrated in Fig. 2.8. The figure is a simplified Feynman diagram

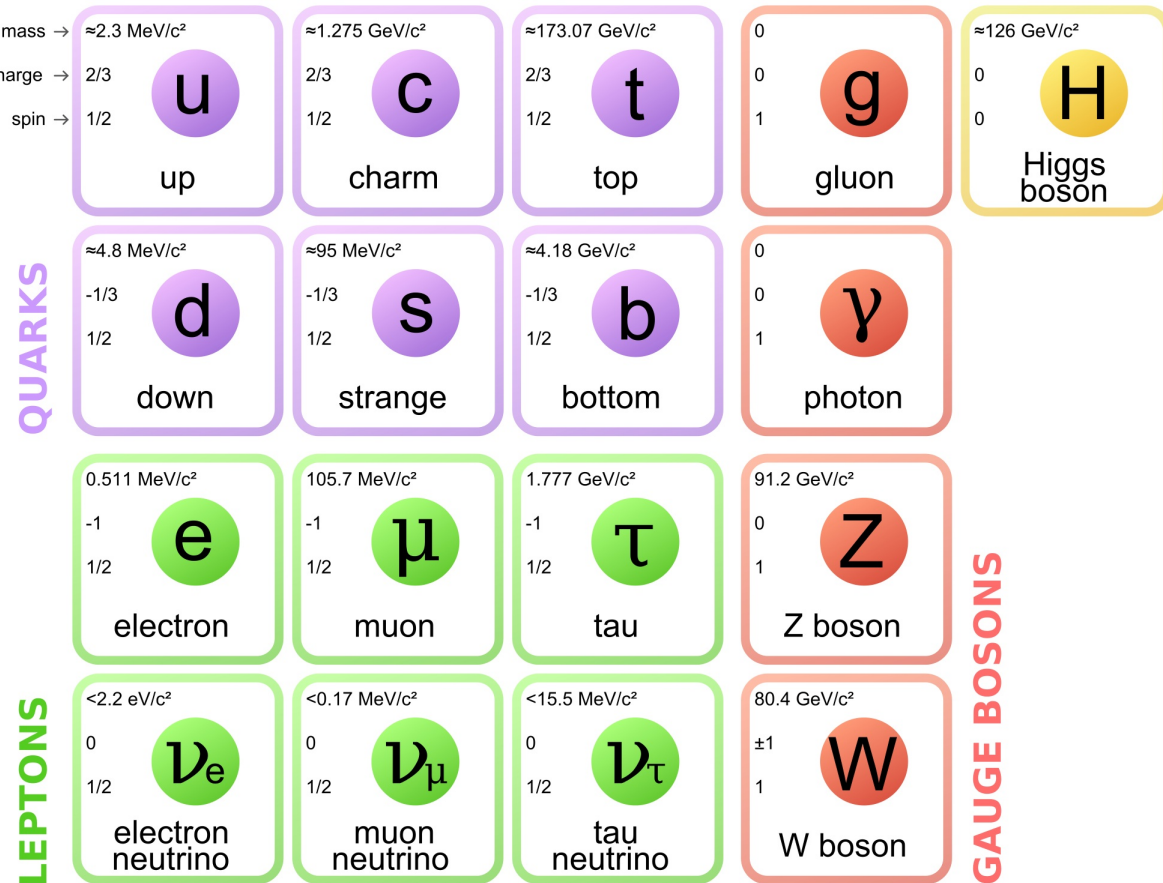


Figure 2.7 The Standard Model (SM) of particle physics. Figure taken from <http://www.quantumdiaries.org/2014/03/14/the-standard-model-a-beautiful-but-flawed-theory/>

- 291 where the arrow of time represents the interaction modes of: **Shake it, Break it, Make it.**
- 292     **Shake it** refers to the direct detection of dark matter. Direct detection interactions start with a  
 293 free DM particle and some SM particle. The DM and SM interact under some elastic or inelastic  
 294 collision and recoil away from each other. The DM remains in the dark sector and imparts some  
 295 momentum onto the SM particle. The hope is that the momentum imparted onto the SM particle  
 296 is sufficiently high enough to pick up with highly sensitive instruments. Because we cannot create  
 297 the DM in the lab, a direct detection experiment must wait until DM is incident on the detector.  
 298 Most direct detection experiments are therefore placed in low-background environments with inert  
 299 detection media like the noble gas Xenon. [14]
- 300     **Make it** refers to the production of DM from SM initial states. The experiment starts with  
 301 particles in the SM. These SM particles are accelerated to incredibly high energies and then collided

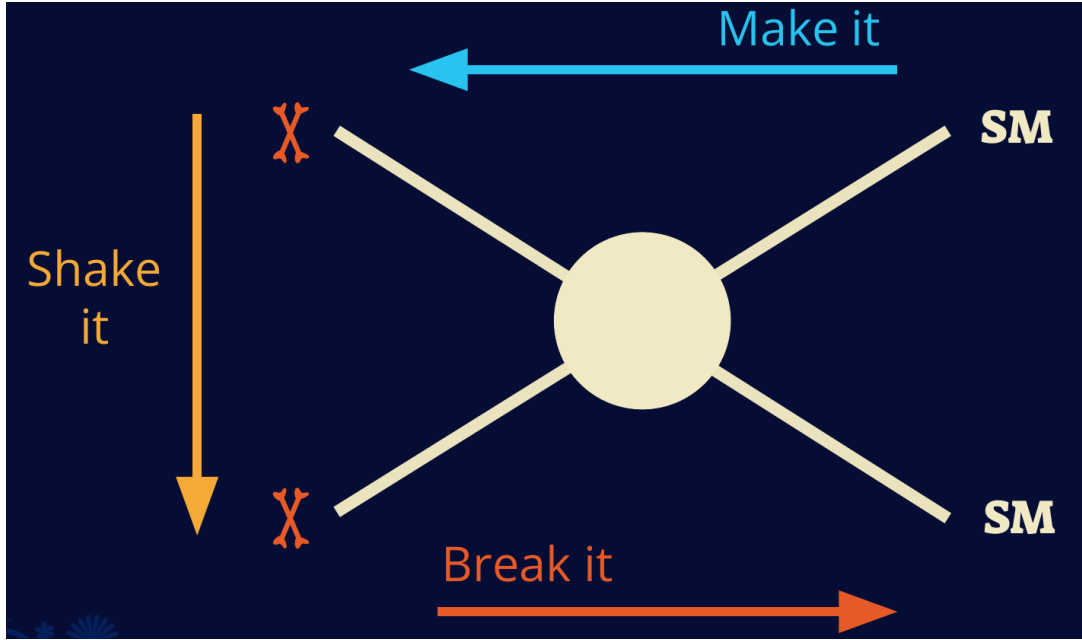


Figure 2.8 Simplified Feynman diagram demonstrating different ways DM can interact with SM particles. The 'X's refer to the DM particles whereas the SM refer to fundamental particles in the SM. The large circle in the center indicates the vertex of interaction and is purposely left vague. The colored arrows refer to different directions of time as well as their respective labels. The arrows indicate the initial and final state of the DM -SM interaction in time.

302 with each other. In the confluence of energy, DM hopefully emerges as a byproduct of the SM  
 303 annihilation. Often it is the collider experiments that are able to generate energies high enough  
 304 to probe DM production. These experiments include the world-wide collaborations ATLAS and  
 305 CMS at CERN where protons are collided together at extreme energies. The DM searches however  
 306 are complex. DM likely does not interact with the detectors and lives long enough to escape the  
 307 detection apparatus of CERN's colliders. This means any DM production experiment searches for an  
 308 excess of events with missing momentum or energy in the events. An example event with missing  
 309 transverse momentum is shown in Fig. 2.9. The missing momentum with no particle tracks implies  
 310 a neutral particle carried the energy out of the detector. However, there are other neutral particles  
 311 in the SM, like neutrons or neutrinos, so any analysis have to account for SM signatures of missing  
 312 momentum. [15]

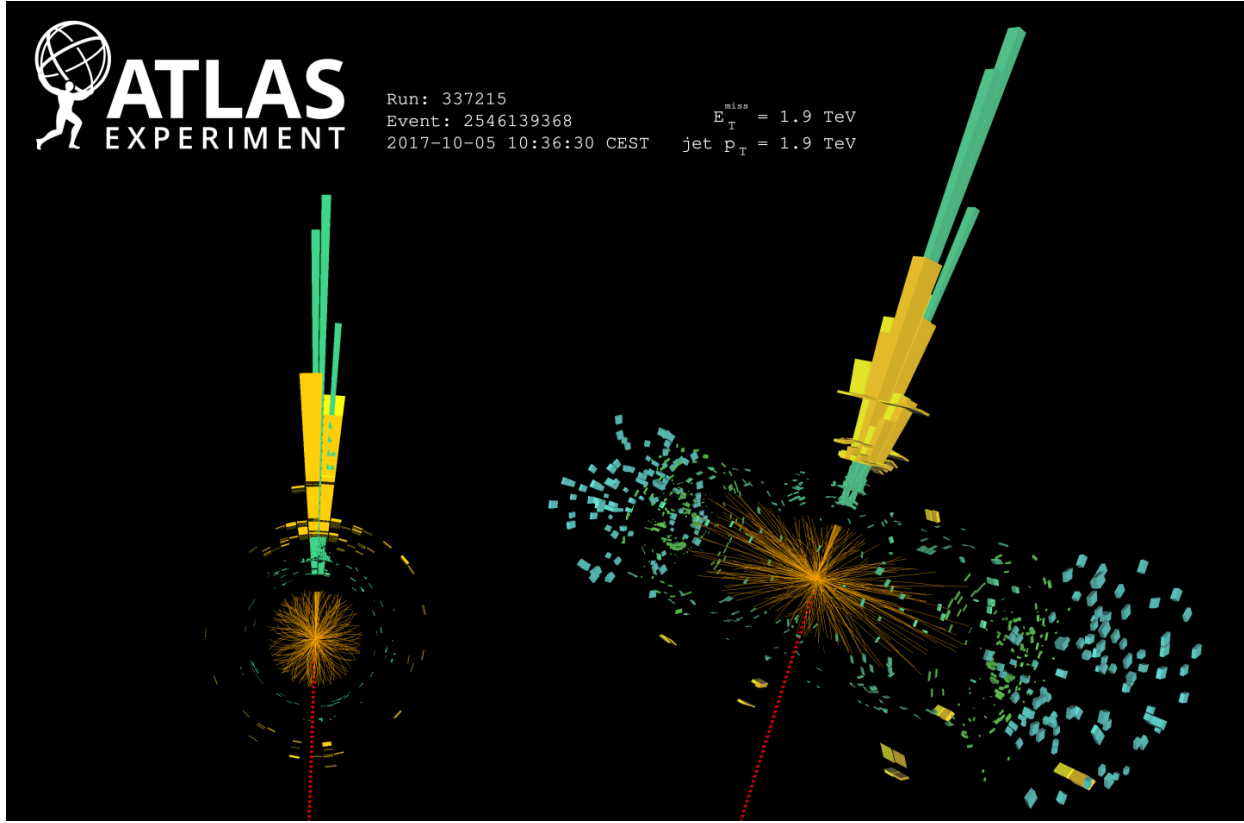


Figure 2.9 A single jet event in ATLAS detector from 2017 [16]. Jet momentum observed to be 1.9 TeV. Missing transverse momentum observed to be 1.9 TeV as the initial momentum of the event was 0. Implied MET is shown as a red dashed line in event display.

### 313 2.4.2 Break it: Standard Model Signatures of Indirect Dark Matter Searches

314     **Break it** refers to the creation of SM particles from the dark sector, and it is the primary focus  
 315     of this thesis. The interaction begins with DM or in the dark sector. The hypothesis is that this  
 316     DM will either annihilate with itself or decay and produce a SM byproduct. This method is often  
 317     referred to the Indirect Detection of DM because we have no lab to directly control or manipulate the  
 318     DM. Therefor most DM primary observations will be performed from observations of known DM  
 319     densities among the astrophysical sources. The strength is that we have the whole of the universe  
 320     and it's 13.6 billion year lifespan to use as the detector or particle accelerator. Additionally, locations  
 321     of dark matter are also well understood since it was astrophysical observations that presented the  
 322     problem of DM in the first place.

323     However, anything can happen in the universe. There are many difficult to deconvolve back-

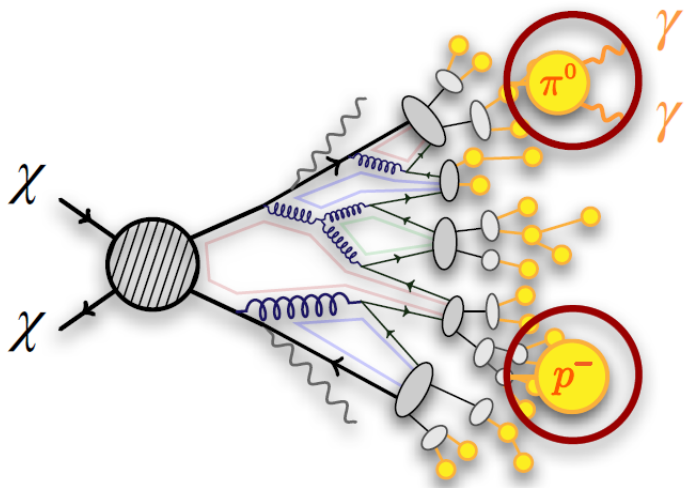


Figure 2.10 More detailed pseudo-Feynman diagram of particle cascade from dark matter annihilation into 2 quarks. The quarks hadronize and down to stable particles like  $\gamma$  or the anti-proton ( $p^-$ ). Diagram pulled from ICRC 2021 presentation on DM annihilation search [17].

324 grounds when searching for DM. Once prominent example is the galactic center. There's a lot of  
 325 DM there since the Milky Way definitely has a lot of DM. But any signal coming from there is hard  
 326 to parse apart from the extreme environment of our supermassive black hole, Sagitarius A\* [18]  
 327 Despite the challenges, any DM model that yields evidence in the other observation two methods,  
 328 **Shake it or Make it** must be corroborated with indirect observations of the known DM sources.  
 329 Without corroborating evidence, DM observation in the lab is hard-pressed to demonstrate that it  
 330 is the model contributing to the DM seen at the universal scale.

331 In the case of WIMP DM, signals are typically described in terms of primary SM particles  
 332 produced from a DM decay or annihilation. The SM initial state particles are then simulated to  
 333 stable final states such as the  $\gamma$ ,  $\nu$ ,  $p$ , or  $e$  which can traverse galactic lengths to reach Earth.

334 Fig. 2.10 shows the quagmire of SM particles that emerges from SM initial states that are not  
 335 stable [17]. There are many different particles with varying energies that can be produced in such an  
 336 interaction. For any arbitrary DM source and stable SM particle, the SM flux from DM annihilating

337 to some neutral particle in the SM,  $\phi$ , from a region in the sky is described by the following

$$\frac{d\Phi_\phi}{dE_\phi} = \frac{\langle\sigma v\rangle}{8\pi m_\chi^2} \frac{dN_\phi}{dE_\phi} \times \int_{\text{source}} d\Omega \int_{l.o.s} \rho_\chi^2 dl(r, \theta') \quad (2.4)$$

338 In Eq. (2.4),  $\langle\sigma v\rangle$  is the velocity-weighted annihilation cross-section of DM to the SM.  $m_\chi$  refers  
339 to the mass of DM, noted with greek letter  $\chi$ .  $\frac{dN_\phi}{dE_\phi}$  is the N particle flux weighted by the particle  
340 energy. An example is provided in Fig. 2.11 for the  $\gamma$  final state. The integrated terms are performed  
341 over the solid angle,  $d\Omega$ , and line of sight, l.o.s.  $\rho$  is the density of DM for a location  $(r, \theta')$  in the  
342 sky. The terms left of the '×' are often referred to as the particle physics component. The terms on  
343 the right are referred to as the astrophysical component. For decaying DM, the equation changes  
344 to...

$$\frac{d\Phi_\phi}{dE_\phi} = \frac{1}{4\pi\tau m_\chi} \frac{dN_\phi}{dE_\phi} \times \int_{\text{source}} d\Omega \int_{l.o.s} \rho_\chi dl(r, \theta') \quad (2.5)$$

345 In Eq. (2.5),  $\tau$  is the decay lifetime of the DM. Just as in Eq. (2.4), the left and right terms are  
346 the particle physics and the astrophysical components respectively. The integrated astrophysical  
347 component of Eq. (2.4) is often called the J-Factor. Whereas the integrated astrophysical component  
348 of Eq. (2.5) is often called the D-Factor.

349     Exact DM  $\text{DM} \rightarrow \text{SM}$  branching ratios are not known, so it is usually assumed to go 100%  
350 into a SM particle/anti-particle. Additionally, when a DM annihilation or decay produces one of  
351 the neutral, long-lived SM particles ( $\nu$  or  $\gamma$ ), the particle can be traced back to a DM source. For  
352 DM above GeV energies, there are very few SM processes that can produce particles with such a  
353 high energy. Seeing such a signal would almost certainly be an indication of the presence of dark  
354 matter. The universe fortunately provides us with the largest volume and lifetime ever for a particle  
355 physics experiment.

## 356 2.5 Sources for Indirect Dark Matter Searches

357     We of course have to know where to look. Thankfully, we have a good idea of where. The  
358 first detection of DM relied on optical observations. Since then, we've developed new techniques  
359 to find DM dense regions. As described in Section 2.3.1, many DM dense regions were through  
360 observing galactic rotation curves. Our Milky Way galaxy is among DM dense regions discovered,

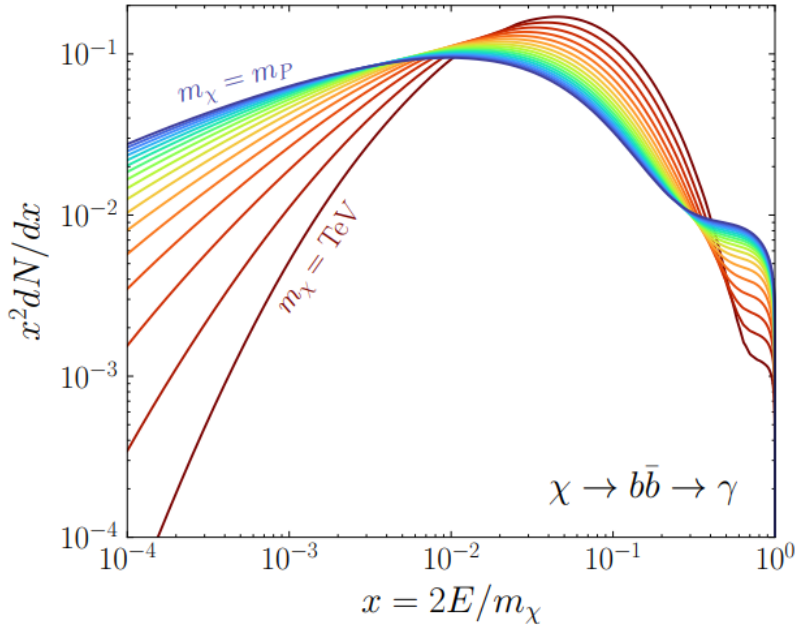


Figure 2.11 Dark Matter (DM) decay spectrum for  $b\bar{b}$  initial state and  $\gamma$  final state. Redder spectra are for larger DM masses. Bluer spectra are light DM masses.  $x$  is a unitless factor defined as the ratio of the mass of DM,  $m_\chi$ , and the final state particle energy  $E_\gamma$ . Figure from [19].

and it is the largest nearby DM dense region to look at. Additionally, the DM halo surrounding the Milky Way is somewhat clumpy [18]. There are regions in the DM halo of the Milky Way that have more DM than others they have captured gas over time. In some cases these sub-haloes were dense enough to host stars. These apparent sub galaxies are known was dwarf spheroidal galaxies and are the main sources studied in this thesis. Each source type comes with different trade offs. Galactic Center studies will be very sensitive to the assume distribution of DM. The central DM density can very substantially as demonstrated in Fig. 2.12. At small r, the differences in DM densities can be 3-4 orders of magnitude.

Dwarf Spheroidal Galaxies (dSph's) studies suffer from uncertainties in the DM density less than the galactic center studies. This is mostly from their diminutive size being smaller than the angular resolution of most  $\gamma$ -ray observatories [18]. The DM content dSph's are typically determined with the virial theorem, Eq. (2.1), and are usually majority DM [18] in mass. DSph's tend to be ideal sources to look at for DM searches. Their environments are fairly quiet with little

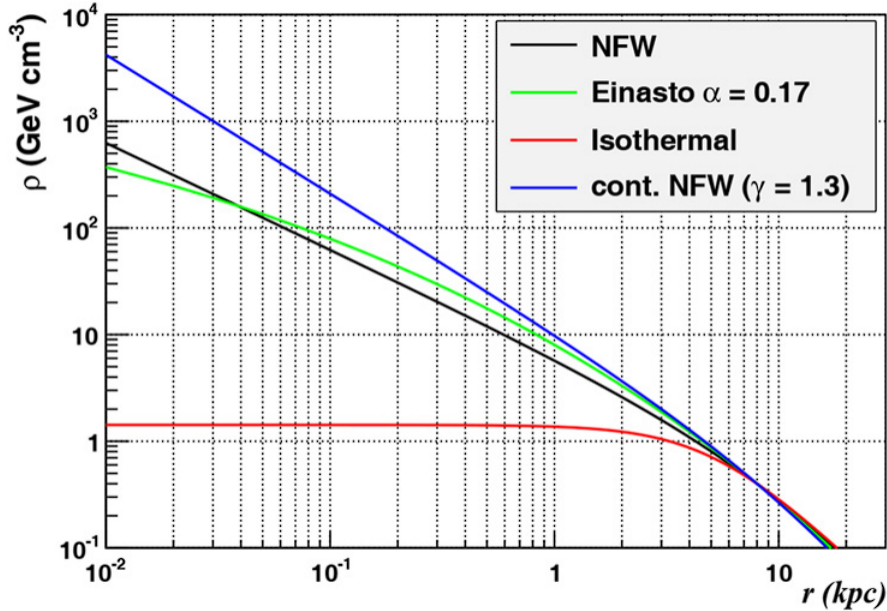


Figure 2.12 Different dark matter density profiles compared. Some models produce very large densities at small  $r$  [20].

374 astrophysical backgrounds. Unlike the galactic center, the most active components of dSph's are  
 375 the stars within them versus a violent accretion disc around a black hole. All this together means  
 376 that dSph's are among the best sources to look at for indirect DM searches. dSph's are the targets  
 377 of focus for this thesis.

## 378 2.6 Multi-Messenger Dark Matter

379 Astrophysics entered a new phase in the past few decades that leverages our increasing sensitivity  
 380 to SM channels and general relativity (GR). Up until the 21st century, astrophysical observations  
 381 were done with photons ( $\gamma$ ) only. Astrophysics with this 'messenger' is fairly mature now. Novel  
 382 observations of the universe have since only adjusted the sensitivity of the wavelength of light  
 383 that's observed. Gems like the CMB [11], and more have ultimately been observations of different  
 384 wavelengths of light. Multi-messenger astrophysics proposes using other SM particles such the  
 385  $p^{+/-}$ , or  $\nu$  or gravitation waves predicted by general relativity.

386 The experiments LIGO had a revolutionary discovery in 2016 with the first detection of a binary  
 387 black hole merger [21]. This opened the collective imagination entirely to observing the universe

388 through gravitational waves. There's also been a surge of interest in the neutrino ( $\nu$ ) sector. IceCube  
 389 demonstrated that we are sensitive to neutrinos in regions that correlate with significant photon  
 390 emmission like the galactic plane [22]. Neutrinos, like gravitational waves and light, travel mostly  
 391 unimpeded from their source to our observatories. This makes pointing to the oringinating source  
 392 of the these messengers much easier than it is for cosmic rays that are almost always deflected from  
 393 their source.

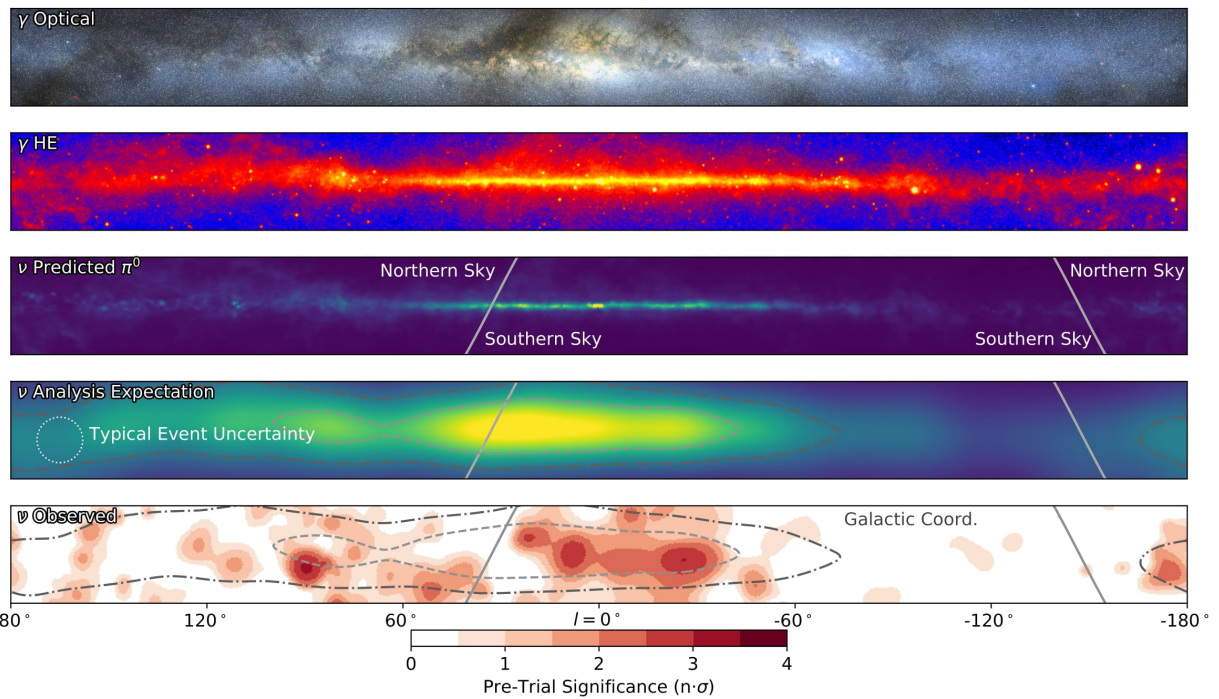


Figure 2.13 The Milky Way Galaxy in photons ( $\gamma$ ) and neutrinos ( $\nu$ ) [22]. Galactic center is at  $l=0^\circ$ and is the brightest region in all panels. (top) An Optical color image of the Milky Way galaxy seen from Earth. Clouds of gas and dust obscure some of the light from stars. (2nd down) Integrated flux of  $\gamma$ -rays observed by the Fermi-LAT telescope [23]. (middle) Expected neutrino emmision that corresponds with Fermi-LAT observations. (2nd up) Expected neutrino emmision profile after considering detector systematics of IceCube. (bottom) Observed neutrino emmision from region of the galactic plane. Substantial neutrino emmision is detected.

394 The recent result from IceCube, shown in Fig. 2.13, proves that we can make obervations under  
 395 different messenger regimes. The top two panels are the appearance of the galactic plane to different  
 396 wavelengths of light. Some sources are more apparent in some panels, while others are not. The  
 397 IceCube collaboration recently published a groundbreaking result of the Milky Way in neutrinos.

398 This new channel is potentially very powerful because neutrinos are readily able to penetrate see  
 399 through gas and dust in the Milky Way. This new image also refines our understanding of how high  
 400 energy particles are accelerated since the fit to IceCube data prefers one standard model process  
 401 over the other [22].

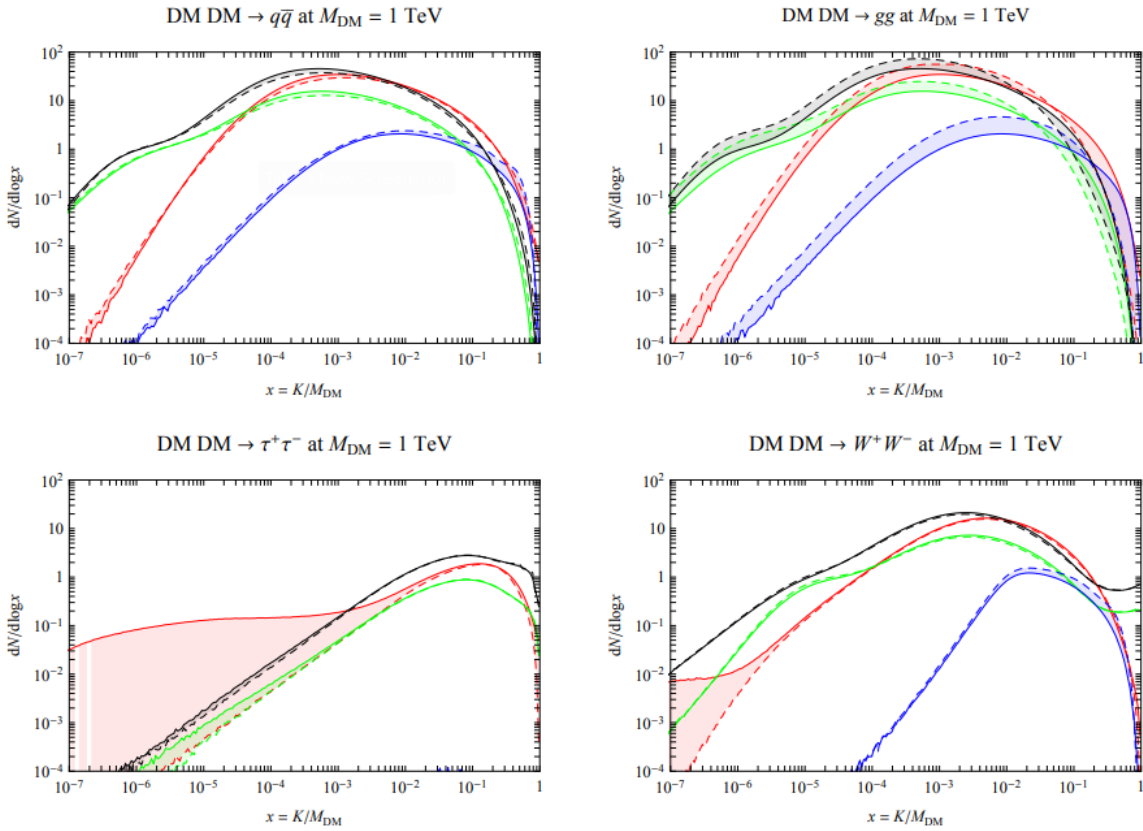


Figure 2.14 Dark Matter annihilation spectra for different final state particle and standard model annihilation channels [24]. Photons (red),  $e^\pm$  (green),  $\bar{p}$  (blue),  $\nu$  (black).

402 Exposing our observations to more cosmic messengers greatly increases our sensitivity to rare  
 403 processes. In the case of DM, Fig. 2.14, there are many SM particles produced in a dark matter  
 404 annihilation. Among the final state fluxes are gammas and neutrinos. Charged particles are also  
 405 produced however they would not likely make it to Earth since they will be deflected by magnetic  
 406 fields between the source and Earth. This means observatories that can see the neutral messengers  
 407 are especially good for DM searches and for combining data for a multi-messenger DM search.

## CHAPTER 3

### DETECTING HIGH ENERGY NEUTRAL MESSENGERS

409 **3.1 Cherenkov Radiation**

410 **3.2 HAWC**

411 **3.3 IceCube**

412 **3.4 Opportunities to Combine for Dark Matter**

## **CHAPTER 4**

413

### **HIGH ALTITUDE WATER CHERENKOV (HAWC) OBSERVATORY**

414 **4.1 The Detector**

415 **4.2 Events Reconstruction and Data Acquisition**

416 **4.2.1 G/H Discrimination**

417 **4.2.2 Angle**

418 **4.2.3 Energy**

419 **4.3 Remote Monitoring**

420 **4.3.1 ATHENA Database**

421 **4.3.2 HOMER**

422

## CHAPTER 5

### ICECUBE NEUTRINO OBSERVATORY

423 **5.1 The Detector**

424 **5.2 Events Reconstruction and Data Acquisition**

425 **5.2.1 Angle**

426 **5.2.2 Energy**

427 **5.3 Northern Test Site**

428 **5.3.1 PIgeon remote dark rate testing**

429 **5.3.2 Bulkhead Construction**

## CHAPTER 6

### COMPUTATIONAL TECHNIQUES IN PARTICLE ASTROPHYSICS

431 **6.1 Neural Networks for Gamma/Hadron Separation**

432 **6.2 Parallel Computing for Dark Matter Analyses**

**CHAPTER 7****GLORY DUCK**

## **CHAPTER 8**

### **NU DUCK**

434

435

## BIBLIOGRAPHY

- 436 [1] Anne M. Green. “Dark matter in astrophysics/cosmology”. In: *SciPost Phys. Lect.*  
 437 *Notes* (2022), p. 37. doi: [10.21468/SciPostPhysLectNotes.37](https://doi.org/10.21468/SciPostPhysLectNotes.37). URL: <https://scipost.org/10.21468/SciPostPhysLectNotes.37>.
- 439 [2] Bing-Lin Young. “A survey of dark matter and related topics in cosmology”. In: *Frontiers*  
 440 *of Physics* 12 (Oct. 2016). doi: <https://doi.org/10.1007/s11467-016-0583-4>.  
 441 URL: <https://doi.org/10.1007/s11467-016-0583-4>.
- 442 [3] Gianfranco Bertone, Dan Hooper, and Joseph Silk. “Particle dark matter: evidence,  
 443 candidates and constraints”. In: *Physics Reports* 405.5 (2005), pp. 279–390. ISSN:  
 444 0370-1573. doi: <https://doi.org/10.1016/j.physrep.2004.08.031>. URL:  
 445 <https://www.sciencedirect.com/science/article/pii/S0370157304003515>.
- 446 [4] Gianfranco Bertone and Dan Hooper. “History of dark matter”. In: *Rev. Mod. Phys.*  
 447 90 (4 Aug. 2018), p. 045002. doi: [10.1103/RevModPhys.90.045002](https://doi.org/10.1103/RevModPhys.90.045002). URL: <https://link.aps.org/doi/10.1103/RevModPhys.90.045002>.
- 449 [5] Fritz Zwicky. “The Redshift of Extragalactic Nebulae”. In: *Helvetica Physica Acta* 6.  
 450 (1933), pp. 110–127. doi: [10.5169/seals-110267](https://doi.org/10.5169/seals-110267).
- 451 [6] Vera C. Rubin and Jr. Ford W. Kent. “Rotation of the Andromeda Nebula from a Spectro-  
 452scopic Survey of Emission Regions”. In: *ApJ* 159 (Feb. 1970), p. 379. doi: [10.1086/150317](https://doi.org/10.1086/150317).
- 454 [7] K. G. Begeman, A. H. Broeils, and R. H. Sanders. “Extended rotation curves of spiral galaxies: dark haloes and modified dynamics”. In: *Monthly Notices of the Royal Astronomical Society* 249.3 (Apr. 1991), pp. 523–537. ISSN: 0035-8711. doi: [10.1093/mnras/249.3.523](https://doi.org/10.1093/mnras/249.3.523). eprint: <https://academic.oup.com/mnras/article-pdf/249/3/523/18160929/mnras249-0523.pdf>. URL: <https://doi.org/10.1093/mnras/249.3.523>.
- 459 [8] *Different types of gravitational lenses*. website. Feb. 2004. URL: <https://esahubble.org/images/heic0404b/>.
- 461 [9] P. Tisserand et al. “Limits on the Macho content of the Galactic Halo from the EROS-2  
 462 Survey of the Magellanic Clouds”. In: *A&A* 469.2 (2007), pp. 387–404. doi: [10.1051/0004-6361:20066017](https://doi.org/10.1051/0004-6361:20066017). URL: <https://doi.org/10.1051/0004-6361:20066017>.
- 464 [10] Douglas Clowe et al. “A Direct Empirical Proof of the Existence of Dark Matter”. In: *apjl*  
 465 648.2 (Sept. 2006), pp. L109–L113. doi: [10.1086/508162](https://doi.org/10.1086/508162). arXiv: [astro-ph/0608407](https://arxiv.org/abs/astro-ph/0608407) [[astro-ph](#)].
- 467 [11] Planck Collaboration and N. et. al. Aghanim. “Planck 2018 results I. Overview and the  
 468 cosmological legacy of Planck”. In: *A&A* 641 (2020). doi: [10.1051/0004-6361/2018](https://doi.org/10.1051/0004-6361/2018)

- 469 33880. URL: <https://doi.org/10.1051/0004-6361/201833880>.
- 470 [12] Wenlong Yuan et al. “A First Look at Cepheids in a Type Ia Supernova Host with JWST”. In: *The Astrophysical Journal Letters* 940.1 (Nov. 2022). doi: [10.3847/2041-8213/ac9b27](https://doi.org/10.3847/2041-8213/ac9b27). URL: <https://dx.doi.org/10.3847/2041-8213/ac9b27>.
- 473 [13] Wendy L. Freedman. “Measurements of the Hubble Constant: Tensions in Perspective”. In: *The Astrophysical Journal* 919.1 (Sept. 2021), p. 16. doi: [10.3847/1538-4357/ac0e95](https://doi.org/10.3847/1538-4357/ac0e95). URL: <https://dx.doi.org/10.3847/1538-4357/ac0e95>.
- 476 [14] Jodi Cooley. “Dark Matter direct detection of classical WIMPs”. In: *SciPost Phys. Lect. Notes* (2022), p. 55. doi: [10.21468/SciPostPhysLectNotes.55](https://doi.org/10.21468/SciPostPhysLectNotes.55). URL: <https://scipost.org/10.21468/SciPostPhysLectNotes.55>.
- 479 [15] “Search for new phenomena in events with an energetic jet and missing transverse momentum in  $pp$  collisions at  $\sqrt{s} = 13$  TeV with the ATLAS detector”. In: *Phys. Rev. D* 103 (11 July 2021), p. 112006. doi: [10.1103/PhysRevD.103.112006](https://doi.org/10.1103/PhysRevD.103.112006). URL: <https://link.aps.org/doi/10.1103/PhysRevD.103.112006>.
- 483 [16] *Jetting into the dark side: a precision search for dark matter*. website. July 2020. URL: <https://atlas.cern/updates/briefing/precision-search-dark-matter>.
- 485 [17] Celine Armand et. al. “Combined dark matter searches towards dwarf spheroidal galaxies with Fermi-LAT, HAWC, H.E.S.S., MAGIC, and VERITAS”. In: *Proceedings of Science*. Vol. 395. Mar. 2022. doi: <https://doi.org/10.22323/1.395.0528>.
- 488 [18] Tracy R. Slatyer. “Les Houches Lectures on Indirect Detection of Dark Matter”. In: *SciPost Phys. Lect. Notes* (2022), p. 53. doi: [10.21468/SciPostPhysLectNotes.53](https://doi.org/10.21468/SciPostPhysLectNotes.53). URL: <https://scipost.org/10.21468/SciPostPhysLectNotes.53>.
- 491 [19] Christian W Bauer, Nicholas L. Rodd, and Bryan R. Webber. “Dark matter spectra from the electroweak to the Planck scale”. In: *Journal of High Energy Physics* 2021.1029-8479 (June 2021). doi: [https://doi.org/10.1007/JHEP06\(2021\)121](https://doi.org/10.1007/JHEP06(2021)121).
- 494 [20] Riccardo Catena and Piero Ullio. “A novel determination of the local dark matter density”. In: *Journal of Cosmology and Astroparticle Physics* 2010.08 (Aug. 2010), p. 004. doi: [10.1088/1475-7516/2010/08/004](https://doi.org/10.1088/1475-7516/2010/08/004). URL: <https://dx.doi.org/10.1088/1475-7516/2010/08/004>.
- 498 [21] B. P. Abbott et al. “Observation of Gravitational Waves from a Binary Black Hole Merger”. In: *Phys. Rev. Lett.* 116 (6 Feb. 2016), p. 061102. doi: [10.1103/PhysRevLett.116.061102](https://doi.org/10.1103/PhysRevLett.116.061102). URL: <https://link.aps.org/doi/10.1103/PhysRevLett.116.061102>.
- 501 [22] R. Abbasi et. al. “Observation of high-energy neutrinos from the Galactic plane”. In: *Science* 380.6652 (June 2023), pp. 1338–1343.

- 503 [23] NASA Goddard Space Flight Center. *Fermi's 12-year view of the gamma-ray sky*. website.  
504 2022. URL: <https://svs.gsfc.nasa.gov/14090>.
- 505 [24] Marco Cirelli et al. “PPPC 4 DM ID: a poor particle physicist cookbook for dark matter  
506 indirect detection”. In: *Journal of Cosmology and Astroparticle Physics* 2011.03 (Mar.  
507 2011), p. 051. DOI: [10.1088/1475-7516/2011/03/051](https://doi.org/10.1088/1475-7516/2011/03/051). URL: <https://dx.doi.org/10.1088/1475-7516/2011/03/051>.  
508